DFT/ECP Study of C−H Activation by (PCP)Ir and (PCP)Ir(H)$_2$ (PCP = η^3-1,3-C$_6$H$_3$(CH$_2$PR$_2$)$_2$). Enthalpies and Free Energies of Associative and Dissociative Pathways†

Karsten Krogh-Jespersen,* Margaret Czerw, Mira Kanzelberger, and Alan S. Goldman*

Department of Chemistry, Rutgers, The State University of New Jersey, New Brunswick, New Jersey 08903, USA

Received June 17, 2000

(PCP)Ir(H)$_2$ (PCP = η^3-1,3-C$_6$H$_3$(CH$_2$PR$_2$)$_2$) complexes are highly effective catalysts for the dehydrogenation of alkanes; in particular, they are the first efficient molecular catalysts for alkane dehydrogenation that do not require a sacrificial hydrogen acceptor. Using density functional theory/effective core potential methods, we have examined C−H bond cleavage in alkanes and arenes by both (PCP)Ir and (PCP)Ir(H)$_2$. C−H addition to the dihydride is accompanied by loss of H$_2$; both associative and dissociative pathways for this exchange reaction have been examined. The energetic barrier ($\Delta E^{\ddagger}$) for associative displacement of H$_2$ by benzene is much lower than the barrier for a dissociative pathway involving initial loss of H$_2$; however, the pathways have very comparable free energy barriers ($\Delta G^{\ddagger}$). Extrapolation to the higher temperatures, bulkier phosphine ligands, and the alkane substrates used experimentally leads to the conclusion that the pathway for the "acceptorless" dehydrogenation of alkanes is dissociative. For hydrocarbon/hydrocarbon exchanges, which are required for transfer−dehydrogenation, dissociative pathways are calculated to be much more favorable than associative pathways. We emphasize that it is the free energy, not just the internal energy or enthalpy, that must be considered for elementary steps that show changes in molecularity.

1. INTRODUCTION

The use of effective core potentials (ECP's) to eliminate explicit consideration of inner, atomic core electrons—electrons considered to be "chemically unimportant"—is a well-established computational electronic structure technique,[1] which has found numerous impressive applications in the study of transition metals.[2] Many of the recent advances in density functional theory (DFT) have had particular impact in studies of organometallic reaction chemistry.[3] Thus, the combination of ECP and DFT methods offers a powerful approach toward the detailed understanding of many aspects concerning the structure and reactivity of organometallic systems. The ability to extract highly accurate thermodynamic and kinetic data from DFT/ECP electronic structure calculations is a particularly valued asset, especially given the dearth of high-quality experimental data available for the energetic parameters of organometallic reactions. Reliable and accurate predictions of reaction and activation energies provide potentially valuable guidance in determining the factors that control the rates and thermodynamics of organometallic reaction mechanisms, including those relevant to catalysis.[4] Rational optimization of catalysts on the basis of electronic structure calculations is now well within reach.[5]

One of the foremost challenges in the field of catalysis lies in the development of systems for the selective functionalization of hydrocarbons.[6,7] Approaches to the development of homogeneous organometallic catalyst systems for this purpose are typically classified according to their presumed mode of C−H bond activation.[8] Systems that operate via σ-bond metathesis, electrophilic activation, and oxidative addition of the C−H bond are often considered the three major classes, though the boundaries between these modes are probably much less clearly defined than is often suggested. Efforts in our laboratories have focused on the last of these classes, reactions involving the oxidative addition of C−H bonds.

Catalytic pathways involving oxidative addition generally require the conjugate reaction, reductive elimination, to complete the catalytic cycle; i.e., the metal shuttles between two oxidation states varying by two units. Particularly in the case of C−H bond activation, the oxidative couple is generally thought to consist of a "low" and a "moderate" oxidation state. For example, rhodium and iridium have played especially important roles in this area, and proposed cycles generally involve M(I)/M(III) couples.[6,7] However, the same outcome could in principle be obtained from a fundamentally very different couple incorporating a "high" oxidation state, e.g., Ir(III)/Ir(V).[9,10]

Rhodium and iridium complexes containing the moiety ML$_2$X (M = Rh, Ir; L = tertiary phosphine; X = a formally anionic ligand, typically a halide) have proven particularly effective for hydrocarbon functionalization in addition to several well-established catalyses (e.g., hydroformylation, hydrosilation, and, most relevant to the present work, olefin hydrogenation).[11] Recently, complexes containing the tridentate "pincer" ligand 1,3-bis(dialkylphosphinomethyl)-phenyl (PCP = η^3-1,3-C$_6$H$_3$(CH$_2$PR$_2$)$_2$) have been found to

* Corresponding authors. K.K.-J.: Phone: (732) 445-4241. E-mail: krogh@rutchem.rutgers.edu. A.S.G.: Phone: (732) 445-5232. E-mail: goldman@rutchem.rutgers.edu.

† Presented at the 219th ACS National Meeting, San Francisco, March 26, 2000; paper no. COMP 0015.

10.1021/ci000061g CCC: $20.00
Published on Web 10/27/2000

Scheme 1. (PCP)Ir-Catalyzed "Acceptorless" Alkane Dehydrogenation: Possible Associative (**A**) and Dissociative (**D**) Pathways

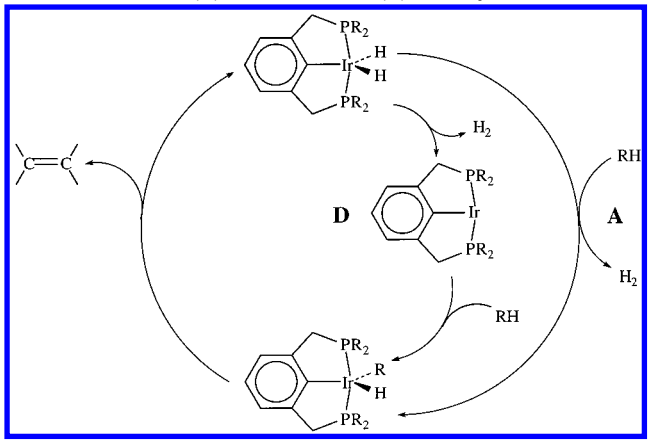

be remarkably effective, and in some cases selective, catalysts for alkane dehydrogenation.[12−15] The degradation and aggregation problems often encountered with ML_2X complexes (X = halide) are avoided through the use of the PCP ligand, which is thermally very stable and does not permit dimerization. We have also shown that replacing a halide with an aryl ring dramatically affects the addition/elimination thermodynamics.[13]

The (PCP)IrH_2-based catalytic system can be operative in either the presence[12,16] or absence[13a,b] of a sacrificial alkene acceptor. A series of elementary reactions forming a possible catalytic mechanism for "acceptorless" alkane dehydrogenation by (PCP)Ir$(H)_2$ is presented in Scheme 1. The dissociative pathway (D) proposes initial reductive elimination of H_2 to afford the three-coordinate, 14-electron (PCP)-Ir complex, followed by C−H bond cleavage to give a five-coordinate, 16-electron Ir(III) alkyl−hydride complex. An associative pathway (A) could involve initial hydrocarbon oxidative addition (C−H bond cleavage) by (PCP)Ir$(H)_2$ to form a seven-coordinate, 18-electron Ir(V) alkyl−trihydride complex which eliminates H_2 to produce the 16-electron Ir-(III) alkyl−hydride complex. Along either pathway, β-hydride elimination from the Ir(III) alkyl−hydride affords the alkene product and regenerates (PCP)Ir$(H)_2$. A series of possible associative and dissociative pathways for (PCP)Ir-catalyzed alkane transfer−dehydrogenation are outlined in Scheme 2.

Here we present DFT/ECP computational results on some of the elementary reactions appearing in Schemes 1 and 2 using alkanes and benzene as substrates. Our focus is on the initial steps leading to formation of the alkyl hydride Ir(III) complex and the respective energetic requirements for associative and dissociative pathways.

2. COMPUTATIONAL METHODS

It is well appreciated that accurate thermodynamic and kinetic parameters are difficult to compute for organometallic molecular systems.[17] In particular, such quantities cannot be predicted within an independent particle, single-determinant Hartree−Fock type approach and, to achieve reliable results, electron correlation must be included in the applied computational methods. In this work, we employ the DFT[18] method along with the B3LYP hybrid functionals for the evaluation of the two-electron exchange-correlation energies ($E_{XC} = E_X + E_C$). The three-parameter hybrid exchange

Scheme 2. (PCP)Ir-Catalyzed Alkane Transfer−Dehydrogenation: Possible Associative (**A**) and Dissociative (**D**) Pathways

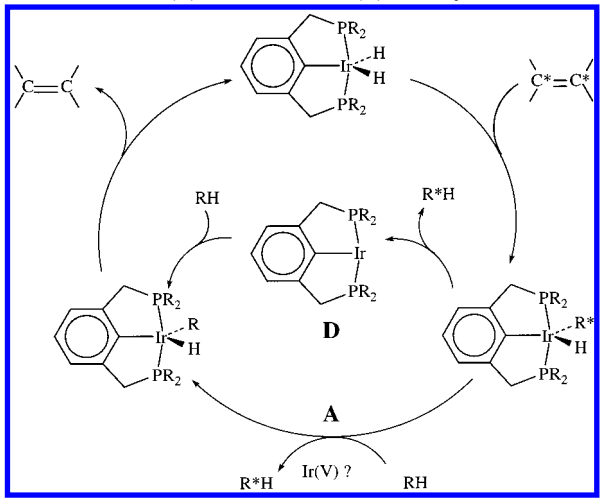

functional proposed by Becke,[19] which incorporates some exact Hartree−Fock exchange, is used for E_X, and E_C is produced by the nonlocal correlation functional of Lee, Yang, and Parr.[20]

The Hay−Wadt relativistic, small-core ECP and corresponding basis sets (split-valence double-ζ) were used for the Ir atom (LANL2DZ model).[21] This 60-electron ECP releases the penultimate valence electrons ($5s^25p^6$ for Ir) for explicit coverage by basis functions along with the valence electrons ($6s^25d^7$). We used all-electron, full double-ζ plus polarization function basis sets for the second- and third-row elements C (Dunning−Huzinaga D95(d))[22a] and P (McLean-Chandler).[22b] Hydrogen atoms in H_2 or the hydrocarbon, which formally become hydrides in the product complexes, were described by the triple-ζ plus polarization 311G(p) basis set;[23] regular hydrogen atoms in alkyl or aryl groups (including PCP) carried a double-ζ quality 21G basis set.[24]

Reactant, transition state, and product geometries were fully optimized using gradient methods[25] and the combination of ECP and basis sets described above (B3LYP/BasisA). The stationary points were characterized further by normal-mode analysis. The (unscaled) vibrational frequencies formed the basis for the calculation of vibrational zero point energy (ZPE) corrections. Thermodynamic corrections were made to convert from purely electronic reaction or activation energies (ΔE, $\Delta E^{\ddagger}$; no ΔZPE) to enthalpies and free energies (ΔH, $\Delta H^{\ddagger}$; ΔG, $\Delta G^{\ddagger}$; ΔZPE included, $T = 298$ K, $P = 1$ atm).[26] Additional single-point calculations at the B3LYP level used a more extended basis set for Ir in which the default LANL2DZ 6p functions were replaced by the functions reoptimized by Couty and Hall,[27] and sets of diffuse d functions (exponent = 0.07) and f functions (exponent = 0.938)[28] were added (B3LYP/BasisB). The B3LYP/BasisB electronic energy−enthalpy−free energy conversions were made in a purely additive fashion based on the data already derived at the B3LYP/BasisA level. Energy data from the B3LYP/BasisB calculations will be used throughout the text. All calculations were executed using the GAUSSIAN 98 series of computer programs.[29]

Our computational model for (PCP)Ir has methyl groups attached to the phosphorus atoms (i.e., $PR_2 = P(CH_3)_2$), a compromise between the use of hydrogen atoms and the alkyl

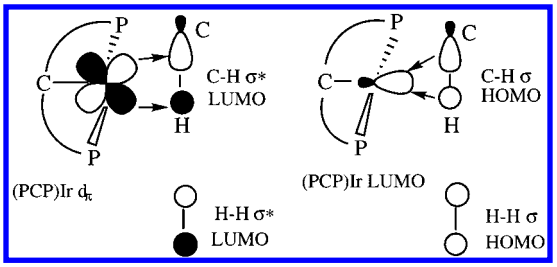

Figure 1. Favorable orbital interactions for addition of H−H or C−H bonds to (PCP)Ir.

groups actually employed in the catalytic systems (^{i}Pr or ^{t}Bu). Methyl groups capture most of the electronic effects imparted by the larger alkyl groups, but they obviously cannot fully model the steric bulk exerted by these groups.[30,31]

2.1. Oxidative Addition of R−H (R = H, CH_3, C_2H_5, C_3H_7, C_6H_5) to (PCP)Ir: Energetics and Product Structures. The two limiting Jahn−Teller structures available to singlet 14-electron ML_3 or ML_2L' fragments with a metal d^8 electronic configuration may be characterized as T- and Y-shaped, respectively.[32] The tridentate PCP ligand enforces a T structure on singlet (PCP)Ir (C_2 symmetry) and a formal ground state electronic configuration $d_{xy}(2)d_{xz}(2)d_{yz}(2)$-$d_{z^2}(2)d_{x^2-y^2}(0)$ (the Ir−C bond defines the *y*-axis; Ir, P, P, and C(PCP) approximately lie in the *xy*-plane). The triplet state of lowest energy ($d_{z^2} \rightarrow d_{x^2-y^2}$ excitation) maintains C_2 symmetry, but it lies more than 35 kcal/mol above the singlet state and will not be considered further in this work.

Addition of an R−H molecule to (PCP)Ir (eq 1) with the

$$\text{(PCP)Ir} + \text{R}-\text{H} \rightarrow \text{(PCP)Ir(R)(H)} \qquad (1)$$

formation of Ir−R and Ir−H bonds formally oxidizes the metal atom from Ir(I) to Ir(III). The transformation from a 14-electron three-coordinate fragment to a 16-electron five-coordinate complex is fully allowed by orbital symmetry (see Figure 1).[32] The LUMO of the three-coordinate fragment is a σ^*-type hybrid orbital composed from the $5d_{x^2-y^2}$, 6s, and 6p orbitals, which protrudes into the open space at the vacant, in-plane coordination site. This orbital has the correct symmetry and extension to interact strongly with the two electrons occupying the H_2 or C−H σ-orbital. Conversely, one of the doubly occupied, in-plane d orbitals (d_{yz}) has the proper local π-type symmetry and extension to interact with the empty σ^*-orbital of the H_2 or C−H bond. The formation of the Ir−H/Ir−C bonds progresses smoothly as the reactant bond is cleaved.

Assuming a least-motion pathway with H_2 approaching (PCP)Ir side-on in the *yz*-plane, the addition reaction may produce trigonal-bipyramidal (TBP) products with the hydrogens cis (Y-shape) or trans (T-shape); the latter structure could also be considered a square pyramid (SQP) in which the phenyl moiety of the PCP ligand occupies the apical position[33] or an octahedron with an empty coordination site. The two structures differ in the occupancies of the metal d orbitals (d^6 configuration). The Y-shaped structure formally has a $d_{xy}(2)d_{xz}(2)d_{y^2-z^2}(2)d_{yz}(0)d_{x^2}(0)$ configuration, whereas the T-shape has $d_{xy}(2)d_{xz}(2)d_{yz}(2)d_{y^2-z^2}(0)d_{x^2}(0)$ (the C(PCP)−Ir bond defines the *y*-axis; C(PCP)−Ir−H−H lie in the *yz*-plane). Addition of R−H (R = CH_3, C_2H_5, C_3H_7, C_6H_5) to (PCP)Ir inevitably leads to structures that exhibit various degrees of distortion from TBP toward SQP coordination with the hydride approaching an apical position (Table 1).

Table 1. Selected Structural Parameters (Bond Lengths in Å, Angles in deg) from the Optimized (PCP)Ir(R)(H) Product Geometries (B3LYP/BasisA)

addendum H−R	structural variable				
	Ir−H	Ir−C(R)	Ir−C-(PCP)[a]	H−Ir−C-(PCP)	C(R)−Ir−C-(PCP)
H−H (Y)	1.593		2.120	150.9	
H−H (T)	1.679		2.012	92.2	
H−CH_3	1.568	2.160	2.080	137.0	151.9
H−C_2H_5	1.563	2.163	2.112	132.7	156.8
H−C_3H_7	1.559	2.160	2.124	131.1	158.6
H−$CH(CH_3)_2$	1.560	2.175	2.127	131.3	157.1
H−C_6H_5	1.539	2.118	2.102	94.7	173.7

[a] 1.979 Å in (PCP)Ir.

Table 2. Computed (B3LYP/BasisA or B3LYP/BasisB at B3LYP/BasisA Optimized Geometries) Thermodynamic Data for the Reaction (PCP)Ir + R−H → (PCP)Ir(R)(H)[a]

addendum H−R	B3LYP/BasisA				B3LYP/BasisB			
	ΔE	ΔH	ΔS	ΔG	ΔE	ΔH^b	ΔS	ΔG^b
H−H (Y shape)	−24.1	−22.3	−27	−14.4	−26.7	−25.0	−27	−17.0
H−H (T Shape)	−16.9	−15.7	−28	−7.4	−17.2	−16.1	−28	−7.8
H−CH_3	1.5	0.1	−31	9.2	−1.5	−2.8	−31	6.4
H−C_2H_5	3.6	2.4	−38	13.6	1.1	−0.2	−38	11.1
H−C_3H_7	4.2	2.7	−37	13.7	1.3	−0.2	−37	10.9
H−$CH(CH_3)_2$	5.7	4.1	−37	15.0	3.2	1.6	−37	12.5
H−C_6H_5	−6.1	−7.4	−31	1.7	−8.6	−9.9	−31	−0.8

[a] Reaction energies (ΔE), enthalpies (ΔH) and free energies (ΔG) are in units of kcal/mol; reaction entropies (ΔS) are in eu (cal/mol·deg). [b] Evaluated by adding the ΔH and ΔG corrections obtained at the B3LYP/BasisA level to ΔE obtained at the B3LYP/BasisB level.

Computed energies pertaining to reaction 1 are shown in Table 2. The dihydrogen addition reaction is strongly exothermic ($\Delta H = -25.0$ kcal/mol) with the most stable product, the Y-shaped TBP isomer, featuring the characteristic highly acute H−M−H angle in the equatorial plane (∼60°, Table 1).[34] The T-shaped TBP (PCP)Ir$(H)_2$ product has an H−Ir−H angle of almost 180° (175.5°) and is calculated to be 9 kcal/mol higher in enthalpy than the Y-shaped isomer. The T−Y difference in ΔG is also about 9 kcal/mol, and the T-shaped isomer will not be considered further, since its concentration at equilibrium relative to that of the Y-isomer will be miniscule.

In contrast, oxidative addition of the simplest alkane, methane, to (PCP)Ir is almost thermoneutral ($\Delta H = -2.8$ kcal/mol) and the product attains a distorted SQP geometry in which the hydride has moved considerably toward an apical position ($\angle$HIrC(PCP) ∼ 137°, $\angle$HIrC(CH_3) ∼ 151°; Table 1). The angles around Ir show both the HIrC(PCP) and C(R)IrC(PCP) angles changing by about 5° further in the direction of SQP coordination as the alkyl chain length increases. In accord with considerable experimental precedent,[6,8,35] the thermodynamic favorability of alkane C−H bond addition decreases as follows: CH_4 > 1° > 2°. The decreased favorability with increasing chain length (methane vs ethane and propane) or branching (primary vs secondary C−H bond breaking in propane) may be attributable to an increase in steric electronic energy (Pauli repulsion), which arises in the reaction product from unfavorable orbital overlaps among filled alkyl ligand and metal orbitals.[36]

Importantly, we compute that addition of benzene (PhH) to (PCP)Ir ($\Delta H = -9.9$ kcal/mol) is substantially more favorable than addition of alkanes (Table 2). The coordination around Ir in the phenyl−hydride product is distinctly SQP with ∠HIrC(PCP) ∼ 95° and ∠C(Ph)IrC(PCP) ∼ 174°. The Ir−Ph bond length is 0.04−0.05 Å less than the Ir−alkyl bond lengths, indicating stronger Ir−C(ligand) interactions with phenyl, presumably due to favorable π-type interactions with the aryl group and/or a lesser degree of unfavorable π-type interactions than with the alkyl groups.

A comparison of reaction energy values (Table 2) shows a general decrease in ΔH relative to ΔE of slightly more than 1 kcal/mol for all the hydrocarbon additions examined here. This change arises primarily from differences in vibrational zero point energies between the two reactant molecules and the product. The reaction energy changes from ΔH to ΔG are more substantial (∼9−11 kcal/mol), however, and strongly disfavor the reactions as there is an entropic penalty when the two molecules combine. In the case of benzene addition to (PCP)Ir, the computed ΔG value is slightly negative (−0.8 kcal/mol), whereas for all alkane additions ΔG is distinctly positive and in the range 6−12 kcal/mol.

The product of benzene addition to (PCP)Ir (where PCP is the bis(*tert*-butylphosphino) derivative) has been observed experimentally.[37] No evidence of free (PCP)Ir is observed in solutions of (PCP)Ir(Ph)H; thus ΔG for benzene addition must be negative. It is difficult to accurately establish the lower limit for the equilibrium constant, since product decomposition occurs in the absence of free benzene and spectroscopic detection of small concentrations of such an intermediate would be difficult due to the fact that exchange is occurring rapidly at or near ambient temperature. At −30 °C, however, exchange is slow and we can conservatively estimate the equilibrium constant to be <0.001, corresponding to $\Delta G_{-30} < -3.3$ kcal/mol for benzene addition to (PCP)-Ir. If an entropy change of ca. −25 eu is assumed (two particles going to one), we can extrapolate the limit to 25 °C as $\Delta G_{25} < -1.9$ kcal/mol.

$$\text{(PCP)Ir(Ph)H} \rightleftarrows \text{(PCP)Ir} + \text{PhH} \qquad K < 0.001 \text{ at } -30\ ^\circ\text{C} \quad (2)$$

We have established that the exchange process proceeds dissociatively, i.e., via elimination of benzene from (PCP)-Ir(Ph)H.[37] The kinetic barrier to elimination, $\Delta G^{\ddagger}_{\text{elim}}$, is found to be 13.9 kcal/mol at −4 °C. Assuming that the reverse reaction (benzene addition) occurs at a (very fast) rate of 10^8 M^{-1} s^{-1} or slower, we can estimate a lower limit for addition, $\Delta G^{\ddagger}_{\text{addn}} \geq 5.8$ kcal/mol at −4 °C. Since $\Delta G_{\text{addn}} = \Delta G^{\ddagger}_{\text{addn}} - \Delta G^{\ddagger}_{\text{elim}}$, we obtain $\Delta G_{\text{addn}} > -8.1$ kcal/mol at −4 °C or $\Delta G_{\text{addn}} > -7.4$ kcal/mol at 25 °C. Thus, ΔG_{addn} at 25 °C appears experimentally bracketed between −1.9 and −7.4 kcal/mol.

The availability of this estimate provides an opportunity to assess the quality of the absolute energetics computed. The comparison between experimental and computed free energy changes is seen to be favorable, in particular with B3LYP/BasisB ($\Delta G_{\text{addn}} = -0.8$ kcal/mol). To make a more proper comparison, we should compute ΔG with the reference state approximating that for the solution phase (1 mol/L, as opposed to the 1 atm ideal gas phase pressure chosen as the default in the calculations). A change in pressure to 24 atm reduces the computed ΔG to −2.7 kcal/mol. This value is within the experimental range and is, at worst, ca. 5 kcal/mol above the experimental value. Although this, of course, does not by any means guarantee that all such reaction energies will be equally accurate, the agreement is impressive and strongly suggestive of the high accuracy achievable in these types of DFT/ECP calculations.

Table 3. Computed Activation Parameters (B3LYP/BasisA or B3LYP/BasisB at B3LYP/BasisA Optimized Geometries) for the Reaction (PCP)Ir + R−H → (PCP)Ir(R)(H)[a]

addendum	B3LYP/BasisA				B3LYP/BasisB			
H−R	$\Delta E^{\ddagger}$	$\Delta H^{\ddagger}$	$\Delta S^{\ddagger}$	$\Delta G^{\ddagger}$	$\Delta E^{\ddagger}$	$\Delta H^{\ddagger a}$	$\Delta S^{\ddagger}$	$\Delta G^{\ddagger a}$
H−CH_3	8.5	6.7	−32	16.2	6.2	4.5	−32	13.9
H−C_2H_5	10.2	8.2	−37	19.2	8.2	6.1	−37	17.2
H−C_3H_7	9.9	8.0	−38	19.3	8.0	6.1	−38	17.4
H−$CH(CH_3)_2$	13.7	11.5	−41	23.6	11.4	9.2	−41	21.3
H−C_6H_5	0.5	−1.4	−39	10.2	−1.8	−3.7	−39	7.9

[a] Activation energies ($\Delta E^{\ddagger}$), enthalpies ($\Delta H^{\ddagger}$), and free energies ($\Delta G^{\ddagger}$) are in kcal/mol; activation entropies ($\Delta S^{\ddagger}$) are in eu (cal/mol·deg). [b] Evaluated by adding the $\Delta H^{\ddagger}$ and $\Delta G^{\ddagger}$ corrections obtained at the B3LYP/BasisA level to $\Delta E^{\ddagger}$ obtained at the B3LYP/BasisB level.

Transition metal complexes with a three-coordinate d^8 configuration are typically highly reactive,[38,39] and considering the reaction energy data presented in Table 2, we expect at most low activation energy barriers for oxidative R−H addition to (PCP)Ir. The spherical symmetry of the H 1s orbitals makes it possible not only to achieve Ir−H orbital overlap early, but also to maintain strong overlap throughout a concerted addition process (Figure 1). In contrast, the directionality of the sp^3-type hybrid used by C in C−H bonding makes orbital following more difficult and tends to induce barriers to bond cleavage.[40] Indeed, for R−H = H−H, a transition state could not be located on the electronic energy surface for the addition to (PCP)Ir. Moderate enthalpic activation barriers are encountered for the addition of alkanes (Table 3), ranging in magnitude from $\Delta H^{\ddagger} = 4.5$ kcal/mol (H−CH_3) to $\Delta H^{\ddagger} = 9.2$ kcal/mol (H−$CH(CH_3)_2$). In accordance with Hammond's principle,[41] the activation energy increases as the reaction endoergicity increases. The calculations predict that addition of benzene, a moderately exothermic reaction (Table 2), proceeds without a barrier on the enthalpy surface.

The electronic structure calculations refer to an idealized gas phase path involving only the two reactant molecules, and they neglect all dynamical aspects and solvation effects. It is thus possible that small barriers exist in solution even for dihydrogen or benzene addition to (PCP)Ir. Since ΔG for the reactions differ from ΔH by 9−12 kcal/mol, distinct activation barriers, spanning the range of 8 kcal/mol (benzene) to 21 kcal/mol (propane), exist on the free energy surfaces for all hydrocarbon additions.

2.2. Oxidative Addition of C_6H_6 to (PCP)Ir$(H)_2$ and (PCP)Ir(C_6H_5)H: Energetics and Product Structures. The (PCP)Ir$(H)_2$ complexes are the first solution phase catalysts reported to effect high-turnover dehydrogenation of alkanes without the use of a hydrogen acceptor.[13] Presumably, a critical segment of the reaction cycle (Scheme 1) is represented by the following equation:

$$\text{(PCP)Ir(H)}_2 + \text{R−H} \rightleftarrows \text{(PCP)Ir(R)H} + \text{H}_2 \qquad (3)$$

Table 4. Computed (B3LYP/BasisA or B3LYP/BasisB) Energies for the Reactions $(PCP)Ir(H)_2 + C_6H_6 \rightarrow (PCP)Ir(Ph)(H_2)(H)$ and $(PCP)Ir(Ph)(H) + C_6H_6 \rightarrow (PCP)Ir(Ph)_2(H_2)$[a]

	B3LYP/BasisA				B3LYP/BasisB			
	ΔE	ΔH	ΔS	ΔG	ΔE	ΔH^b	ΔS	ΔG^b
product								
A	5.8	5.4	−44	18.5	4.2	3.8	−44	17.0
B	7.2	7.0	−39	18.5	6.3	6.1	−39	17.6
C	9.1	8.8	−45	22.1	7.2	6.8	−45	20.2
$(PCP)Ir(Ph)_2(H_2)$	7.2	7.3	−53	23.2	5.0	5.2	−53	21.1
transition states								
C → **A**	4.9	3.5	−1	3.8	3.6	2.3	−1	2.5
R → **B**	23.2	21.9	−45	35.4	21.5	20.2	−45	33.6
R → **C**	18.1	16.6	−45	30.0	16.5	15.0	−45	28.3

[a] Reaction energies (ΔE), enthalpies (ΔH), and free energies (ΔG) are in units of kcal/mol; reaction entropies (ΔS) are in eu (cal/mol·deg). [a] Evaluated by adding the ΔH and ΔG corrections obtained at the B3LYP/BasisA level to ΔE obtained at the B3LYP/BasisB level.

The mechanism of this reaction may have important implications concerning the rate-determining step and, accordingly, any efforts to further develop the catalyst. In this section, we consider reaction 3 with a focus on benzene as the hydrocarbon. We are not proposing to investigate the catalytic dehydrogenation of benzene. Rather, our choice is based on the fact that the product of reaction 3 is not known for R = alkyl. Indeed, the calculations discussed in the above section predict that any such species would be thermodynamically unfavorable with respect to elimination at ambient or higher temperatures. In contrast, we have recently reported the synthesis and characterization of the phenyl analogue, (PCP)Ir(Ph)H,[37] which provides a useful model and allows our computational data to be compared with the results of experiments currently in progress.

The central questions we address are the following: is the mechanism of reaction 3 associative or is elimination of H prior to C−H addition more favorable?[42−44] And if the mechanism is associative, does it involve the intermediacy of Ir(V) species such as $(PCP)Ir(Ph)(H)_3$?

While precedents for a seven-coordinate Ir(V) configuration are well established,[44] all our attempts to locate a classical $(PCP)Ir(Ph)(H)_3$ trihydride resulted in structural collapse to nonclassical Ir(III) dihydrogen complexes of the same composition.[45] We were able to locate minima corresponding to the possible $(PCP)Ir(Ph)(H_2)H$ isomers (**A**, **B**, and **C**). The three minima lie very close in energy ($\Delta\Delta H$

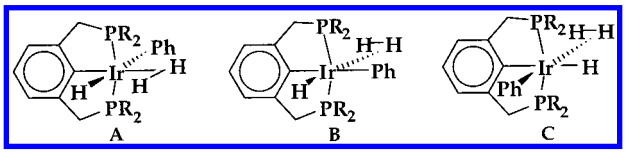

(kcal/mol): **A** (0.0), **B** (2.3), **C** (3.0)) and the reaction energies according to eq 4 are only moderately positive: ΔH

$$(PCP)Ir(H)_2 + C_6H_6 \rightarrow (PCP)Ir(Ph)(H_2)H \qquad (4)$$

= 3.8, 6.1, and 6.8 kcal/mol for formation of **A**, **B**, and **C**, respectively (Table 4).

Transition states (TS) have been located for the formation of **B** and **C** from the reactants (R), $(PCP)Ir(H)_2$ and C_6H_6. These transition states are 15.0 kcal/mol (R → **C**) and 20.2 kcal/mol (R → **B**), respectively, above the reactants on the

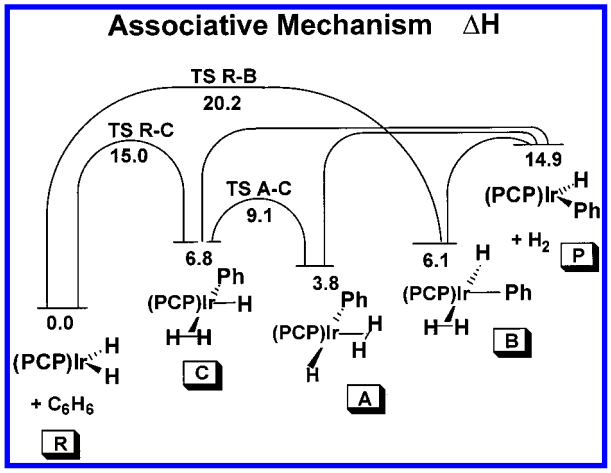

Figure 2. Model associative mechanism: C_6H_6 addition to $(PCP)Ir(H)_2$; ΔH (kcal/mol).

enthalpy surface (Table 4). We have not performed any intrinsic reaction coordinate calculations,[46] but based on geometry and the displacements in the normal mode corresponding to the reaction coordinate, it appears that the located transition state connects the reactants to **C** and not to **A**. In either case, the interconversion of **A** and **C** involves only a very small enthalpy barrier (2.3 kcal/mol with respect to **C**). There is no direct way of attaining structure **B** from either **A** or **C**.

We present relevant enthalpy quantities for a model associative mechanism in Figure 2. To the left, we have the isolated reactants, R = $(PCP)Ir(H)_2 + C_6H_6$, as the zero-point reference. To the right, we have the separated products, P = $(PCP)Ir(Ph)(H) + H_2$, which are computed to lie 14.9 kcal/mol above the reactants. The possible intermediates **A**, **B**, and **C** are 4−7 kcal/mol above the reactants. The last stage of the associative mechanism is the loss of the coordinated H_2 molecule (eq 5) for which we have been

$$(PCP)Ir(Ph)(H_2)(H) \rightarrow (PCP)Ir(Ph)(H) + H_2 \qquad (5)$$

unable to locate a TS from either **A**, **B**, or **C** (in the simulated gas phase). It is possible that small, solvent-cage-induced barriers exist in solution phase (an issue currently under investigation in our group). According to this scheme, a barrier of 15.0 kcal/mol (by coincidence, essentially equal to the overall endothermicity of the reaction, ΔH = 14.9 kcal/mol) must be overcome to yield intermediate **C**, which may dissociatively release H_2 either directly or via prior rearrangement to **A**. Considering that the direct elimination of H_2 from $(PCP)Ir(H)_2$, the first step in a dissociative model, is endothermic by 25.0 kcal/mol (Table 2; Figure 3, left), the associative pathway looks highly attractive. A scheme showing internal energy differences would be essentially superimposable on the enthalpy profile of Figure 2, and any mechanistic conclusions drawn on that basis would be identical.

However, as noted in the discussion of elementary addition reactions to (PCP)Ir, changes in reaction molecularity occur and the landscape is thus very different on the free energy surface (Figure 4). Comparing Figures 2 and 4, we see that the energies of intermediates **A**−**C** and the transition states for their formation have been raised 10 kcal/mol or more relative to the reactants and the products by (unfavorable)

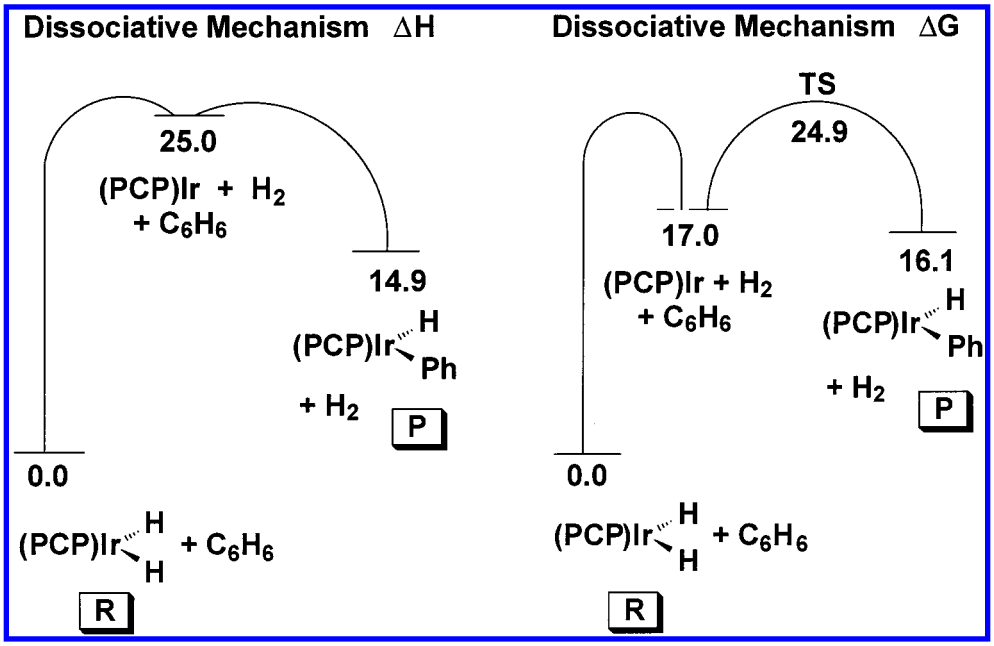

Figure 3. Model dissociative mechanism: C_6H_6 addition to (PCP)Ir(H)$_2$; ΔH (kcal/mol) and ΔG (kcal/mol).

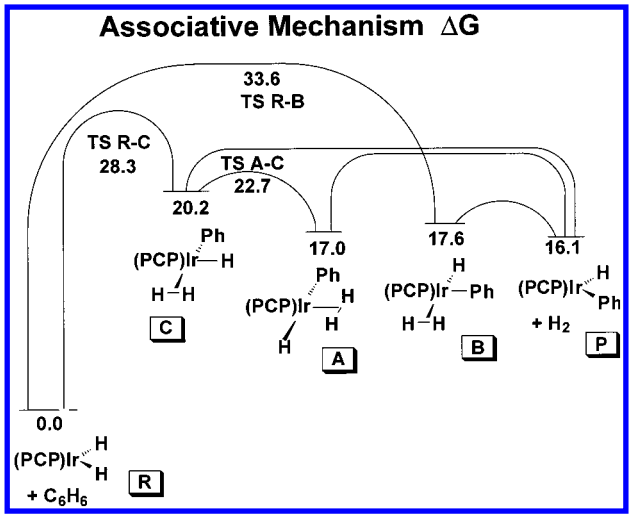

Figure 4. Model associative mechanism: C_6H_6 addition to (PCP)-Ir(H)$_2$; ΔG (kcal/mol).

entropy contributions. The relative positions of reactants and products hardly change ($\Delta G_{rxn} = 16.1$ kcal/mol), but the activation energy for the formation of intermediate **C** (or **A**) from the reactants is a substantial 28.3 kcal/mol on the free energy surface. The dissociative pathway involves a barrier of 24.9 kcal/mol for benzene addition to (PCP)Ir (Table 2; Figure 3, right) and a slightly lower barrier for loss of H_2. The difference between the free energies of activation for the associative and dissociative pathways, 28.3 kcal/mol − 24.9 kcal/mol = 3.4 kcal/mol, corresponds to a factor of ca. 300 favoring the *dissociative* pathway. If we consider that the benzene concentration is ca. 270-fold greater in the liquid than in the gas phase (1 atm), and that there are six C−H bonds per benzene molecule, then the *associative* pathway is actually favored by a very small margin. However, the balance will shift back once again toward the *dissociative* pathway at the higher temperatures relevant to the actual catalytic reactions.

After proper consideration of entropic effects, the barriers to associative and dissociative pathways would thus appear to be quite comparable under experimentally realistic conditions. However, it should be noted that the oxidative addition of alkanes to late transition metal centers is invariably much less favorable than addition of benzene. For example, the differences of 7−13 kcal/mol between benzene and the alkanes considered in the previous section in the context of addition to (PCP)Ir (cf. Table 2) are in good agreement with experimental values reported by Jones, Bergman, and others.[6,35] Actual catalytic acceptorless dehydrogenation systems involve much higher temperatures than 298 K and phosphine ligands much bulkier than methyl, which should preferentially inhibit the addition of alkanes relative to the addition of the (planar) benzene molecule. When these factors are taken into account, the results of this work very strongly suggest that such systems predominantly operate via dissociative loss of H_2.

An exchange reaction closely related to that of eq 3 is shown in eq 6, where one hydrocarbon displaces another

$$(PCP)Ir(R)H + R^*{-}H \rightarrow (PCP)Ir(R^*)H + R{-}H \quad (6)$$

hydrocarbon rather than displacing H_2. As mentioned in the previous section, we find that (PCP)Ir(Ph)H does indeed undergo rapid arene exchange as evidenced by experiments with inequivalent arenes (e.g., benzene and toluene) or by dynamic NMR in pure benzene. Does this exchange of arenes occur via an associative or dissociative path? We calculate that the associative reaction of eq 7, although only endo-

$$(PCP)Ir(Ph)(H) + C_6H_6 \rightarrow (PCP)Ir(Ph)_2(H_2) \quad (7)$$

thermic by 5.2 kcal/mol, is uphill by 21.1 kcal/mol on the free energy surface (Table 4).

The product of eq 7 is a symmetrical species (C_2 symmetry) in which the two phenyl groups flank a dihydrogen molecule situated trans to the PCP ligand, i.e., it is an Ir(III) complex. The activation barriers ($\Delta E^{\ddagger}$, $\Delta H^{\ddagger}$, $\Delta G^{\ddagger}$) for the formation of this species are 20.5, 19.2, and 35.7 kcal/mol, respectively. In contrast, the free energy barrier to elimination of benzene is calculated to be only 8.8 kcal/

mol (combination of data in Tables 2 and 3; Figure 3). Thus, $\Delta G^{\ddagger}$ for the associative exchange pathway is greater by a very wide margin (more than 25 kcal/mol). This is in complete agreement with experimental results, which demonstrate that the exchange rate is independent of the free arene concentration.[37]

Since alkane addition is less favorable than arene addition, the associative pathway for alkane exchange should have an even greater barrier ($\Delta G^{\ddagger} > 35$ kcal/mol). The barrier for alkane elimination, conversely, is even lower than that of benzene elimination ($\Delta G^{\ddagger} = 8.8$ kcal/mol), e.g., 7.5 kcal/mol for methane and 6.5 kcal/mol for propane (Tables 2 and 3). The higher temperatures and greater steric bulk present in the catalytic systems would further increase the already very large advantage of the dissociative pathway for alkane/alkane exchange. Thus, elimination of hydrogenated acceptor (alkane) undoubtedly occurs prior to oxidative addition of the alkane substrate in the transfer−dehydrogenation cycle (path D in Scheme 2).[47]

3. CONCLUDING REMARKS

Both acceptorless dehydrogenation and transfer−dehydrogenation catalyzed by "(PCP)Ir" involve substitution or exchange reactions, either replacement of H_2 by hydrocarbon or a hydrocarbon/hydrocarbon exchange.[12−15] Understanding the pathways of these reactions is a necessary part of developing any comprehensive energy profile, particularly for the acceptorless case in which H_2 loss (whether associative or dissociative) may be rate determining. We have chosen to focus on benzene as a model hydrocarbon, because it permits the comparison of calculations with experimental results on the recently discovered complex, (PCP)Ir(Ph)H.[37]

We find that on both the energy and enthalpy profiles the associative pathway for substitution of H_2 by benzene is significantly more favorable than the dissociative pathway. However, our results emphasize the importance of considering free energies, when evaluating reaction mechanisms, which differ in molecularity. In doing so, we note that the pathways are calculated to possess barriers that are quite comparable, although the dissociative pathway would be favored at the actual temperatures of the catalytic system. Since benzene addition is undoubtedly more favorable than alkane addition, this very strongly suggests that the dissociative pathway is more favorable for reactions of alkanes, the actual substrates for dehydrogenation. The standard ideal gas type treatment typically employed in electronic structure calculations may overemphasize entropic effects and render the corrections from enthalpy to free energy too large, but omitting them in the present discussion of associative vs dissociative mechanisms would clearly lead to a very different and incorrect picture.

The structural and energetic influences exerted by bulky phosphines continue to be of interest. Presumably, increased ligand bulk further enhances the selectivity already calculated for less-substituted C−H groups. It is also possible that sterically bulky phosphines may engender differential enthalpy vs free energy effects and may lead to additional differences between C−H cleavage in alkanes and that in arenes. DFT calculations scale favorably with molecular size and would seem to be the method of choice for further investigations of such "substituent" effects.

ACKNOWLEDGMENT

We gratefully acknowledge the National Science Foundation for financial project support (CHE-9704304) and for a computer equipment grant (DBI-9601851-ARI). We thank Prof. M. B. Hall for communication of results prior to publication.

REFERENCES AND NOTES

(1) (a) Krauss, M.; Stevens, W. J. *Annu. Rev. Phys. Chem.* **1984**, *35*, 357. (b) *Pseudopotential Theory of Atoms and Molecules*; Szazs, L., Ed.; Wiley: New York, 1985. (c) Christiansen, P. A.; Ermler, W. C.; Pitzer, K. S. *Annu. Rev. Phys. Chem.* **1985**, *36*, 407. (d) Kahn, L. R.; Baybutt, P.; Truhlar, D. G. *J. Chem. Phys.* **1976**, *65*, 3826.

(2) (a) Frenking, G.; Antes, I.; Böhme, M.; Dapprich, S.; Ehlers, A. W.; Jonas, V.; Neuhaus, A.; Otto, M.; Stegmann, R.; Veldkamp, A.; Vyboishchikov, S. F. *Reviews in Computational Chemistry*; Boyd, D., Lipkowitz. K., Eds.; VCH Publishers: New York, 1996; Vol. 8., pp 63−144. (b) Benson, M. T.; Cundari, T. R.; Lutz, M. L.; Sommerer, S. O. *Reviews in Computational Chemistry*; Boyd, D., Lipkowitz. K., Eds.; VCH Publishers: New York, 1996; Vol. 8., pp 145−202.

(3) (a) Ziegler, T. *Chem. Rev.* **1991**, *91*, 651. (b) *Density-Functional Methods in Chemistry and Materials Science*; Springborg, M., Ed.; John Wiley and Sons, Ltd.: New York, 1997. (c) *Density Functional Methods in Chemistry*; Labanowski, J., Andzelm, J., Eds.; Springer-Verlag: Heidelberg, 1991.

(4) (a) *Theoretical Aspects of Homogeneous Catalysis, Applications of Ab Initio Molecular Orbital Theory*; van Leeuwen, P. W. N. M., van Lenthe, J. H., Morokuma, K., Eds.; Kluwer: Dordrecht, The Netherlands, 1994. (b) *Transition State Modeling for Catalysis*; ACS Symposium Series 721, Truhlar, D. G., Morokuma. K., Eds.; American Chemical Society: Washington, DC, 1998.

(5) Deng, L.; Ziegler, T.; Woo, T. K.; Margl, P.; Fan, L. *Organometallics* **1998**, *17*, 3240−3253. Besenbacher, F.; Chorkendorff, I.; Clausen, B. S.; Hammer, B.; Molenbroek, A. M.; Nørskov, J. K.; Stensgaard, I. *Science* **1998**, *279*, 1913−1915.

(6) Arndtsen, B. A.; Bergman, R. G.; Mobley, T. A.; Peterson, T. H. *Acc. Chem. Res.* **1995**, *28*, 154−162.

(7) Jones, W. D. *Science* **2000**, *287*, 1942−1943.

(8) For an excellent lead reference, see: Bennett, J. L.; Wolczanski, P. T. *J. Am. Chem. Soc.* **1997**, *119*, 10696−10719.

(9) Chen, H.; Schlect, S.; Semple, T. C.; Hartwig, J. F. *Science* **2000**, *287*, 1995−1997.

(10) During the course of this study the first observation of C−H addition to give a M(V) adduct (iridium) was reported: Klei, S. R.; Tilley, T. D.; Bergman, R. G. *J. Am. Chem. Soc.* **2000**, *122*, 1816−1817.

(11) Collman, J. P.; Hegedus, L. S.; Norton, J. R.; Finke, R. G. *Principles and Applications of Organotransition Metal Chemistry*; University Science Books: Mill Valley, CA, 1987; pp 523−576.

(12) (a) Gupta, M.; Hagen, C.; Flesher, R. J.; Kaska, W. C.; Jensen, C. M. *Chem. Commun.* **1996**, 2083−2084. (b) Gupta, M.; Hagen, C.; Kaska, W. C.; Cramer, R. E.; Jensen, C. M. *J. Am. Chem. Soc.* **1997**, *119*, 840−841.

(13) (a) Xu, W.; Rosini, G. P.; Gupta, M.; Jensen, C. M.; Kaska, W. C.; Krogh-Jespersen, K.; Goldman, A. S. *Chem. Commun.* **1997**, 2273−2274. (b) Liu, F.; Goldman, A. S. *Chem. Commun.* **1999**, 655−656. Krogh-Jespersen, K.; Goldman, A. S. *Transition State Modeling for Catalysis*, ACS Symposium Series 721, Truhlar, D. G., Morokuma, K., Eds.; American Chemical Society: Washington, DC, 1998; pp 151−162.

(14) Liu, F.; Pak, E. B.; Singh, B.; Jensen, C. M.; Goldman, A. S. *J. Am. Chem. Soc.* **1999**, *121*, 4086−4087.

(15) Jensen, C. M. *Chem. Commun.* **1999**, 2443−2449.

(16) Liu, F.; Goldman, A. S. *Chem. Commun.* **1999**, 655−656.

(17) (a) Veillard, A. *Chem. Rev.* **1991**, *91*, 743−766. (b) Gordon, M. S. *Modern Electronic Structure Theory*; Yarkony, D. R., Ed.; World Scientific Publishing: Singapore, 1994; pp 311−344. (c) Bauschlicher, C. W., Jr.; Langhoff, S. R.; Partridge, H. *Modern Electronic Structure Theory*; Yarkony, D. R. Ed.; World Scientific Publishing: Singapore, 1994; pp 1280−1374.

(18) Parr, R. G.; Yang, W. *Density-Functional Theory of Atoms and Molecules*; University Press: Oxford, 1989.

(19) Becke, A. D. *J. Chem. Phys.* **1993**, *98*, 5648−5652.

(20) Lee, C.; Yang, W.; Parr, R. G. *Phys. Rev. B* **1988**, *37*, 785.

(21) Hay, P. J.; Wadt, W. R. *J. Chem. Phys.* **1985**, *82*, 299.

(22) (a) Dunning, T. H.; Hay, P. J. In *Modern Theoretical Chemistry*; Schaefer, H. F., III, Ed.; Plenum: New York, 1976; pp 1−28. (b) McLean, A. D.; Chandler, G. S. *J. Chem. Phys.* **1980**, *72*, 5639.
(23) Krishnan, R.; Binkley, J. S.; Seeger, R.; Pople, J. A. *J. Chem. Phys.* **1980**, *72*, 650.
(24) Binkley, J. S.; Pople, J. A.; Hehre, W. J. *J. Am. Chem. Soc.* **1980**, *102*, 939.
(25) Schlegel, H. B. *Modern Electronic Structure Theory*; Yarkony, D. R., Ed.; World Scientific Publishing: Singapore, 1994; pp 459−500.
(26) McQuarrie, D. A. *Statistical Thermodynamics*; Harper and Row: New York, 1973.
(27) Couty, M.; Hall, M. B. *J. Comput. Chem.* **1996**, *17*, 1359.
(28) Ehlers, A. W.; Böhme, M.; Dapprich, S.; Gobbi, A.; Höllwarth, A.; Jonas, V.; Köhler, K. F.; Stegmann, R.; Veldkamp, A.; Frenking, G. *Chem. Phys. Lett.* **1993**, *208*, 111.
(29) Frisch, M. J.; Trucks, G. W.; Schlegel, H. B.; Scuseria, G. E.; Robb, M. A.; Cheeseman, J. R.; Zakrzewski, V. G.; Montgomery, J. A.; Stratmann, R. E.; Burant, J. C.; Dapprich, S.; Millam, J. M.; Daniels, A. D.; Kudin, K. N.; Strain, M. C.; Farkas, O.; Tomasi, J.; Barone, V.; Cossi, M.; Cammi, R.; Mennucci, B.; Pomelli, C.; Adamo, C.; Clifford, S.; Ochterski, J.; Petersson, G. A.; Ayala, P. Y.; Cui, Q.; Morokuma, K.; Mailick, D. K.; Rabuck, A. D.; Raghavachari, K.; Foresman, J. B.; Cioslowski, J.; Ortiz, J. V.; Stefanov, B. B.; Liu, G.; Liashenko, A.; Piskorz, P.; Komaromi, I.; Gomperts, R.; Martin, R. L.; Fox, D. J.; Keith, T.; Al-Laham, M. A.; Peng, C. Y.; Nanayakkara, A.; Gonzalez, C.; Challacombe, M.; Gill, P. M. W.; Johnson, B. G.; Chen, W.; Wong, M. W.; Andres, J. L.; Head-Gordon, M.; Replogle, E. S.; Pople, J. A. *Gaussian 98*, Revision A.5; Gaussian Inc.: Pittsburgh, PA 1998.
(30) Wüllen, C. J. v. *J. Comput. Chem.* **1997**, *18*, 1985−1992.
(31) Wang, K.; Rosini, G. P.; Nolan, S. P.; Goldman, A. S. *J. Am. Chem. Soc.* **1995**, *117*, 5082−5088.
(32) Albright, T. A.; Burdett, J. K.; Whangbo, M. *Orbital Interactions in Chemistry*; John Wiley & Sons: New York, 1985; pp 78−82.
(33) We have not been able to locate SQP-type isomers for (PCP)Ir(H)$_2$ with H in an apical position.
(34) Riehl, J.-F.; Jean, Y.; Eisenstein, O.; Pelissier, M. *Organometallics* **1992**, *11*, 729.
(35) Wick, D. D.; Jones, W. D. *Organometallics* **1999**, *18*, 495−505.
(36) (a) Ziegler, T.; Tschinke, V.; Becke, A. *J. Am. Chem. Soc.* **1987**, *109*, 1351−1358. (b) Ziegler, T.; Tschinke, V.; Versluis, L.; Baerends, E. J.; Ravenek, W. *Polyhedron* **1988**, *7*, 1625−1637.
(37) Kanzelberger, M.; Singh, B.; Czerw, M.; Krogh-Jespersen, K.; Goldman, A. S. *J. Am. Chem. Soc.*, accepted for publication.
(38) Crumpton, D. M.; Goldberg, K. I. *J. Am. Chem. Soc.* **2000**, *122*, 962−963 and references therein.
(39) Harper, T. G. P.; Desrosiers, P. J.; Flood, T. C. *Organometallics* **1990**, *9*, 2523−2528.
(40) (a) Low, J. J.; Goddard, W. A., III. *Organometallics* **1986**, *5*, 609−622. (b) Saillard, J.-Y.; Hoffmann, R. *J. Am. Chem. Soc.* **1984**, *106*, 2006−2026.
(41) Hammond, G. S. *J. Am. Chem. Soc.* **1955**, *77*, 334.
(42) Using computational methods similar to ours, Niu and Hall have calculated energies of reaction 3 for alkane addition (PCP = η^3-1,3-$C_6H_3(CH_2PH_2)_2$) (ref 43). We find that differences between the PCP ligands used, R = H vs R = Me, are not insignificant. Even more importantly, we find that entropy differences play a critical role and thus energies are not sufficient to address this question.
(43) (a) Niu, S. Q.; Hall, M. B. *J. Am. Chem. Soc.* **1999**, *121*, 3992−3999. (b) Niu, S. Q.; Hall, M. B. *Chem. Rev.* **2000**, *100*, 353−405.
(44) Li, S. H.; Hall, M. B.; Eckert, J.; Jensen, C. M.; Albinati, A. *J. Am. Chem. Soc.* **2000**, *122*, 2903−2910 and references therein.
(45) (a) Jessop, P. G.; Morris, R. J. *Coord. Chem. Rev.* **1992**, *121*, 155−284. (b) Lin, Z.; Hall, M. B. *Inorg. Chem.* **1992**, *31*, 4262−4265.
(46) Gonzalez, C.; Schlegel, H. B. *J. Phys. Chem.* **1990**, *94*, 5523.
(47) Energy ($\Delta E^{\ddagger}$) calculations by Hall, concomitant with this work, have independently led to the same conclusion, that alkane/alkane exchange proceeds dissociatively: Hall, M. B., personal communication. Note that, in contrast to the hydrocarbon/H_2 exchange of eq 3, for alkane/alkane exchange (eq 6) the energy barrier ($\Delta E^{\ddagger}$) as well as the free-energy ($\Delta G^{\ddagger}$) barrier is lower for the dissociative than for the associative pathway.

CI000061G